Catalysis Today 156 (2010) 165–172

Contents lists available at ScienceDirect

Catalysis Today

journal homepage: www.elsevier.com/locate/cattod

Evaluation of the water gas shift reaction in a palladium membrane reactor

P. Pinacci[a,*], M. Broglia[a], C. Valli[a], G. Capannelli[b], A. Comite[b]

[a] ERSE, Via Rubattino 54, 20134 Milano, Italy
[b] Dipartimento di Chimica e Chimica Industriale, Università di Genova, Italy

ARTICLE INFO

Article history:
Available online 24 March 2010

Keywords:
Membrane reactor
Palladium composite membrane
Water gas shift
Carbon monoxide conversion

ABSTRACT

The water gas shift (WGS) reaction of a syngas mixture has been carried out in a tubular palladium membrane reactor at a temperature of 410–414 °C. A composite palladium-porous stainless steel membrane, 29 μm thick, obtained by electroless plating, has been first extensively tested with pure gases (H_2, He, CO_2) and syngas mixtures in the 310–455 °C temperature range and up to 800 kPa. Long-term stability of the membrane in H_2 at 400 °C has also been checked over a period of 1200 h. The membrane has been then used for WGS tests in a membrane reactor. The membrane reactor, packed with a pulverized Fe/Cr commercial catalyst, has been operated at a reaction pressure of 100–600 kPa in the counter-current mode, with a nitrogen sweep-gas. The reactor has been fed with a shift gas mixture with a 7.6% CO concentration and H_2O/CO ratio in the 2.7–3.6 range. The membrane reactor was able to achieve up to the 85.0% of CO conversion, while only the 37% as a maximum, was reached with the traditional reactor in the same operating conditions. Up to the 82% of hydrogen has been recovered with a purity exceeding the 97%.

1. Introduction

Membranes are widely studied for pre-combustion capture of CO_2 in integrated gasification combined cycles (IGCC) power plants [1,2]. A lot of efforts are devoted to the development of palladium alloy membranes for CO_2 capture and hydrogen separation from synthesis gas in membrane reactors [3–5]. Due to the considerable cost of palladium, efforts have been made to obtain low thickness deposits on cheaper materials, such as macroporous metals, by various techniques [6–9], including electroless plating [9–12].

Works in the recent past have been mainly focused on water gas shift (WGS) at low temperature (e.g. 250–300 °C) using Pd–Ag alloys [13–16]; high temperature WGS of syngas obtained by coal gasification has not been investigated due to the lack of stability of membranes at such temperatures (500–550 °C); moreover the high concentration of CO in the dry gas (over the 40% by volume), which can adsorb on the membrane surface, has a considerable poisoning effect on H_2 permeation [17–19]. Only a few work dealing with WGS at intermediate temperature (e.g. around 400 °C) can be found in literature [20,21]; both works, however, deal with a syngas produced by steam reforming, while this work focuses on syngas produced in IGCC plants. In addition Pd-membrane used in Refs. [20,21] have been obtained by electroless plating on ceramic supports, while this paper considers Pd-membranes on a metallic support.

Since the stability of Pd membranes on metallic supports up to 400 °C is nowadays sufficiently proved [22–25], based on the above considerations it is interesting to evaluate the performances of a palladium membrane reactor for WGS at such an intermediate temperature [26]; more in detail it can be assumed that the syngas produced in a IGCC plant has already been treated in a conventional high temperature WGS reactor and the CO concentration has been reduced from 40 to 43% below the 8%, so minimizing the poisoning effects on H_2 permeation.

For this purpose a composite palladium-porous stainless steel membrane has been prepared by electroless plating. This membrane has been first extensively tested in pure gases and, thereafter, in a syngas mixture in order to define its performances in terms of permeability and permselectivity.

The long-term stability in H_2 flux has also been assessed. The membrane has been then used for WGS tests at 400 °C in a membrane reactor. In this paper results of the WGS tests are particularly addressed.

2. Experimental

2.1. Membrane preparation

A 29 μm thick composite palladium membrane has been prepared by electroless plating on a stainless steel tubular macroporous support.

The support is a 10 mm O.D. AISI 316L porous tube, with a nominal pore size of 0.1 μm, supplied by Mott Metallurgical Corporation. Nominal pore size is determined by the manufacturer based on a

* Corresponding author. Tel.: +39 02 39925865.
E-mail address: pietro.pinacci@erse-web.it (P. Pinacci).

0920-5861/$ – see front matter © 2010 Elsevier B.V. All rights reserved.
doi:10.1016/j.cattod.2010.02.034

95% rejection of particles with size greater than 0.1 μm. The actual pore size, however is much larger: a mean and maximum value of about 2 and 5 μm, respectively, has been determined by mercury intrusion measurements [27].

Rugosity of the surface is also rather high; the maximum high of the profile is R_y = 31 μm, while the mean rugosity is R_m = 7.2 μm [28].

Two non-porous AISI 316 L tubes were welded at the ends of the porous support in order to allow a gas tight sealing when introducing the membrane in the reactor. The total length of the support is 20 cm and the active length of the porous support is 7.5 cm. The active surface of the membrane is 23.5 cm^2.

Membrane preparation has been performed according to a procedure similar to the one developed by Ma et al. [29] and consists of the following steps:

- Cleaning of the support in an ultrasonic bath with acetone, followed by successive rinsing in water, diluted hydrochloric acid, de-ionized water up to a neutral pH, and acetone.
- Oxidation of the support in a oven with static air at the temperature of 500 °C for two successive cycles of 10 h.
- Activation of the oxidised support by dipping into a stannous chloride solution ($SnCl_2$ 1 g/l in HCl 0.2 N) and a palladium chloride solution ($PdCl_2$ 0.1 g/l in HCl 0.2 N), alternately, for many times. Activation is performed at room temperature at pH < 1 in order to maintain a good salt solubility; the number of dipping cycles depends on the support characteristics. This steps is the most critical since it influence the subsequent deposition of palladium, dimension of grains and ultimately film morphology and stability.
- Deposition of palladium by electroless plating performed in a solution of palladium chloride (3.5 g/l), ammonia (30% solution, 650 ml/l), $EDTANa_2$ (76 g/l) and hydrazine (1 M). Pd plating is obtained by circulating the solution in a reactor where the membrane is immersed and kept in rotation in order to obtained an homogeneous deposit on the external surface and facilitate nitrogen evacuation from the reaction zone; temperature is kept constant (47–50 °C) by a thermostatic bath. Typically 1–2 μm of Pd are deposited for each bath.

At the end of each bath, membrane thickness has been estimated by gravimetric measurements and, thereafter, helium permeance at room temperature has been determined. The membrane has been considered as dense and, consequently, palladium deposition stopped, when helium permeance has been reduced well below 10^{-9} mol/s/m^2/Pa at a transmembrane pressure higher than 600 kPa (see Fig. 1).

2.2. Laboratory pilot loop description

Both permeation and WGS tests where performed in a laboratory pilot loop consisting of:

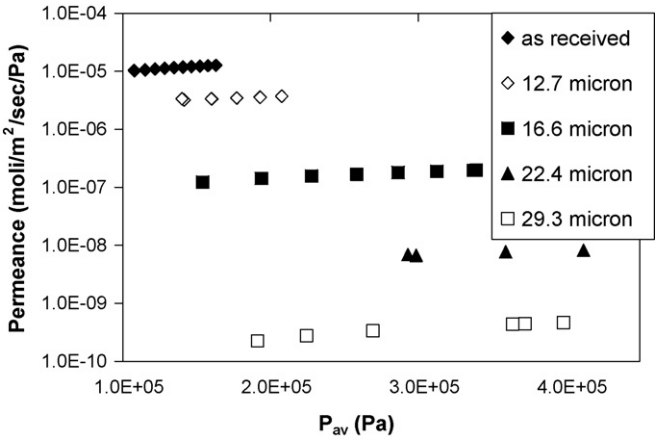

Fig. 1. He permeance at room temperature of the Pd-composite membrane for different Pd layer thicknesses.

- Mass flow controllers (Bronkhorst High Tech) which regulate process gases and permeate feed flow. The water flow is regulated by a liquid mass flow controller (Bronkhorst High Tech); the water tank is pressurized with N_2 to force water in the evaporation section before mixing with other gases.
- An electrically heated oven where process gases and water are heated up to the operating temperature and where the test section is housed.
- A test section consisting of a 316 L stainless steel reactor (20 mm I.D.) where the tubular membrane is housed (see Fig. 2); gas tight sealing is insured by welding the non-porous end of the membrane support to the reactor. Process gases are fed to the shell side of the membrane, while a counter-current sweep gas (N_2), also used as a carrier for gas chromatograph analysis, is fed to the lumen side of the membrane.
- A water trap for water vapour condensation at the exit of the reactor.
- An on-line gas chromatograph (Varian CP-4900) for the analysis of dry gases.
- An acquisition and control system (Agilent model 34970A) of the main process parameters (temperatures, pressures, gas flow rates), interfaced with a computer.

2.3. Tests description

Test performed with the membrane described in Section 2.1 are summarized in Table 1. The membrane has been tested at a temperature ranging from 300 to 455 °C for a total of 2900 h, for 7 cycles along a period of about 10 months.

In each cycle the membrane has been heated up to the operating temperature at a rate of 1 °C/min in a inert gas (He); at the end of the cycle, before cooling down to room temperature the membrane has been flushed with He at pressure of 250 kPa,

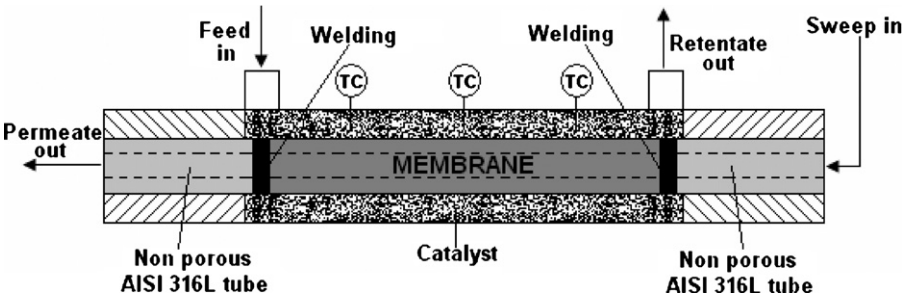

Fig. 2. Scheme of the test section where the membrane is housed.

Table 1
Tests performed with the Pd-composite membrane.

Cycle	Description	T (°C)	Duration (h)
1	Permeation tests with He	20–400	70
2	Permeation tests with pure gases (He, H_2)	310–455	250
3	Permeation tests with pure gases (He, H_2, CO_2)	310–455	250
4	Permeation tests with a WGS gas mixture	400	300
5	Long-term permeation tests with H_2	400	1200
6	WGS tests with a membrane reactor	410–414	216
7	WGS tests with a membrane reactor	410–414	614
	Total		2900

for about 2 h, to purge any H_2 trapped in the palladium lattice. Both at the beginning and at the end of each cycle (except cycle 1, where only He has been fed to check membrane stability at temperature) permeation tests with pure He and H_2 have been performed at the temperature of 400 °C, in order to check membrane performances.

During cycle 2 and 3 permeation tests with pure gases (He, H_2, CO_2) have been performed to determine H_2 permeability and membrane permselectivity in the 310–455 °C range. The permeate side was kept at 1 bar. H_2 flux was determined both with a bubble meter and with on-line chromatographic analysis when a sweep gas (N_2) was used. The permselectivity, at a given temperature and pressure, is defined as the ratio between the permeance of the hydrogen and permeance of the slower permeating gas (He or CO_2).

During cycle 4 permeation tests have been performed at 400 °C with gas mixtures simulating synthesis gas composition (see Table 2) to evaluate any possible detrimental effect of gases such as CO or CO_2 on H_2 permeation. In this latter case hydrogen permeance was calculated by dividing the hydrogen flux by the average hydrogen partial pressure difference over the membrane.

During cycle 5 long-term stability of the membrane at 400 °C has been evaluated by feeding H_2 at a pressure of 250 kPa for 1200 h. H_2 and He permeance have been checked every week in order to evidence any variation in the membrane performance.

During cycle 6 and 7 WGS tests in a membrane reactor have been performed. A Fe/Cr commercial catalyst (GC-3) supplied by Sud-Chemie in 6 × 6 mm tablets has been pulverized and two size fractions, 425–600 and 600–710 μm, respectively, have been separated by screening. The selected catalyst powders have been mixed with an inert powder (α-alumina) with the same size fraction. Specifically 12.7 g of catalyst and 16.0 g of alumina have been charged in the reactor. The catalyst bed extended along the whole length of the membrane, as shown in Fig. 2.

The catalyst and powder mixture have been charged in the annulus of the reactor where the syngas has been fed at 410–414 °C. A sweeping gas (N_2) has been fed in the lumen side of the membrane at atmospheric pressure. Reactor has been operated in the countercurrent mode. Feed pressure has been progressively increased up to 650 kPa in order to remove hydrogen from the reaction zone through the membrane and evaluate the influence on the conversion of the WGS reaction. Both the retentate and the permeate composition have been determined by on-line gas chromatograph measurements.

Table 2
Composition of gas mixtures fed to membrane in cycle 4.

Gas	Composition (% by volume)					
CO	–	4	4	5.5	5.5	7
H_2O	23	12	16	16.5	22	28
H_2	49	53	52	50	46	42
CO_2	28	31	28	28	26.5	23

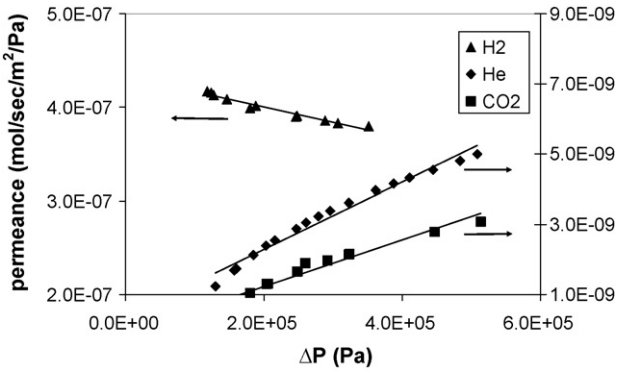

Fig. 3. Permeance of H_2, He and CO_2 measured at 402 °C.

3. Results and discussion

3.1. Permeation tests

Permeation tests with pure gases (H_2, CO_2 and He) in the 310–455 °C range have been performed during cycle 2 and 3 (see Table 1).

Typical results are shown in Fig. 3 where the permeance of each gas at 400 °C as a function of the pressure drop across the membrane is reported. It can be noted that both He and CO_2 permeance increase with pressure difference due to the viscous flow component through the defects (pinholes) in the Pd layer. As expected He permeance is higher than the CO_2 one, due to the presence of a diffusive flux component through defects in the mesoporous range (between 2 and 50 nm), as discussed in Ref. [11].

As a consequence of the above described phenomena, the permselectivity between H_2 and other gases exhibit a decreasing trend as a function of the pressure drop, as shown in Fig. 4. As expected, permselectivity increases with the temperature; moreover differences between CO_2 and He and the temperature effect

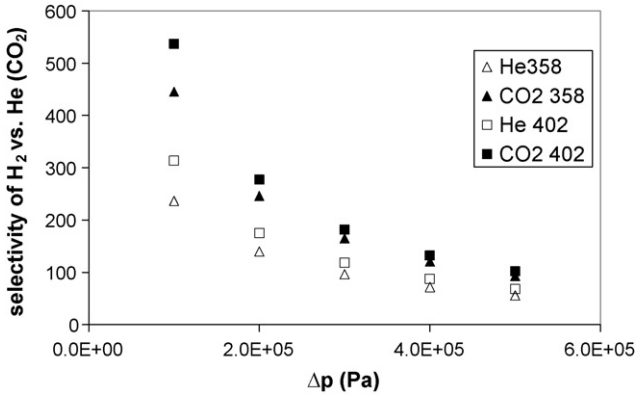

Fig. 4. Selectivity of H_2 versus He (or CO_2), at 358 °C and 402 °C.

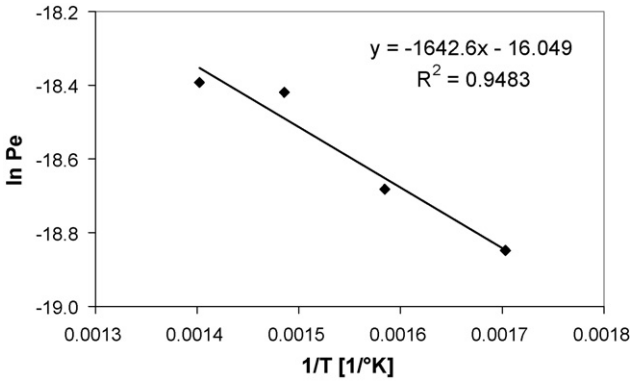

Fig. 5. Arrhenius plot of the permeability of the membrane.

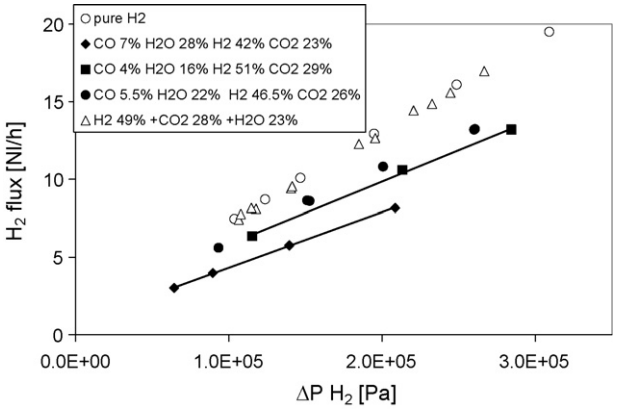

Fig. 6. Hydrogen flux versus the average hydrogen partial pressure difference over the membrane: comparison between measurements with pure H_2 and gas mixtures at 400 °C.

tends to level off while increasing pressure drop, due to the growing relative weight of the viscous flow component.

The decreasing trend of the separation factor has also been reported by Rothenberger et al. [30] for two composite Pd-porous stainless steel membranes, 22 μm thick, similar to the one tested in this work.

Experimental data has been further treated in order to determine the mechanism of hydrogen permeation through the membrane. H_2 flux data has been interpolated with the least square line method, i.e. by minimizing the sum of the square of residuals, according to the following equation:

$$J = \frac{Pe}{L}\left[(p_f)^n - (p_p)^n\right]$$

where J (mol/s/m^2) is the H_2 flux; Pe (mol/s/m/Pa^n) the membrane permeability; L the Pd layer thickness; p_f and p_p the H_2 partial pressure in the feed and in the permeate, respectively.

The best fitting value of the n exponent is 0.60 at 310 °C and 0.56 for temperatures ranging between 358 and 440 °C, indicating that the hydrogen permeation through the membrane is mainly determined by bulk diffusion in the Pd layer. These values can be compared to n values of 0.55 and 0.64 estimated at 400 °C for the two membranes in the above cited work of Rothenberger et al. [30]. Guazzone et al. have also estimated a n value of 0.55 at 400 °C for a composite Pd-porous stainless steel membranes, 33 μm thick [31].

Moreover, if according to the procedure indicate by Guazzone in Ref. [31], the hydrogen flux is depurated from the contribution of the viscous and diffusive flow through defects, the estimated values of n decrease to 0. 55 at 310 °C at to 0.5 at higher temperatures.

Therefore it can be assumed, with a reasonable approximation, that hydrogen permeation through the membrane occurs according to the Sievert law (n = 0.5); the corresponding permeability (Pe) can be expressed by an Arrhenius-type equation:

$$Pe = Pe_0 \exp\left(-\frac{E_a}{RT}\right)$$

where E_a (activation energy) is 13.66 kJ/mol and $Pe_0 = 1.07 \times 10^{-7}$ (mol/m/s/Pa$^{0.5}$) (see Fig. 5).

The activation energy is very close to the value of 13.41 kJ/mol determined by Morreale et al. for bulk palladium membranes [32] and is in good agreement with other literature data [33].

During cycle 4 permeation tests have been performed at 400 °C with gas mixtures simulating synthesis gas composition (see Table 2). Specifically CO concentration has been varied between 4 and 7% and H_2O/CO ratio between 3 and 4.

Results are summarized in Fig. 6, where the measured hydrogen flux is plotted versus the average hydrogen partial pressure difference over the membrane. For comparison, data obtained with pure hydrogen at the beginning and at the end of the cycle are also plotted in the graph. It can be noted that H_2 flux is partially inhibited by the presence of CO, while it remains unchanged in a mixture containing H_2, CO_2 and H_2O. More in detail a flux reduction of the 30% and 40%, approximately, has been measured for CO concentration of the 4–5.5% and 7%, respectively. Moreover no polarization effect has been detected in the tests with the feeds containing CO, due to the low hydrogen recover factor (below the 50%). The observed H_2 flux reduction can be attributed to CO adsorption on the membrane surface and to the consequent reduction of sites available for H_2 dissociation [17–19]; this phenomena is reversible, e.g. H_2 flux returns to the original value when CO flow is stopped [34]. Flux reduction could be more severe for thinner membranes where H_2 dissociation tends to become the rate determining step of the permeation process; in particular Peters et al. reported a H_2 flux reduction of about the 60% in a WGS mixture with the 5.5% of CO, while testing a Pd–Ag membrane, 1.6 μm thick, at 400 °C [19].

During cycle 5 long-term tests in pure H_2 at 400 °C have been performed in order to check membrane stability. Hydrogen flux remained constant up to 1000 h and slightly decreased, 8% approximately, at the end of the test (1200 h). He permeance, besides, remained unchanged until the end of the test.

3.2. WGS tests

Typical compositions of the syngas used for WGS tests are shown in Table 3: CO concentration has been maintained as fixed, while the H_2O/CO ratio has been 3.58 and 2.66, respectively, for the two feed tested, in order to help in preventing any carbon deposition. Total flow rate, and consequently space velocity, has also been kept constant with both feeds. Space velocity, 1400 l kg^{-1} h^{-1}, is inside

Table 3
Typical composition of syngas processed in the membrane reactor.

	CO		CO_2		H_2O		H_2		GHSV	H_2O/CO
	%Vol	Nl/h	%Vol	Nl/h	%Vol	Nl/h	%Vol	Nl/h	l kg^{-1} h^{-1}	
Feed 1	7.6	1.35	23.7	4.2	27.1	4.8	41.6	7.36	1394	3.58
Feed 2	7.6	1.35	26.4	4.7	20.2	3.6	45.8	8.15	1402	2.66

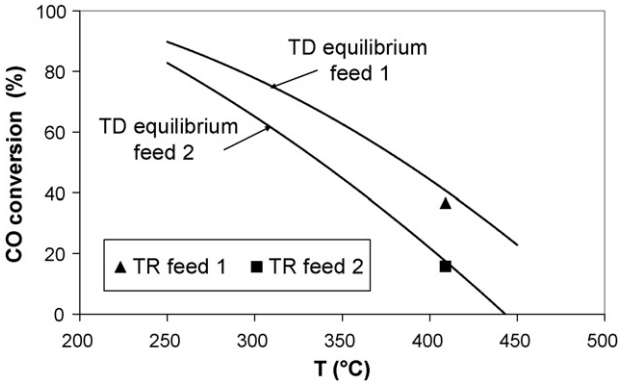

Fig. 7. CO conversion obtained with a traditional reactor (TR) for feed 1 and 2, respectively: comparison with thermodynamic equilibrium data.

the optimum range, 1000–3000, suggested by the catalyst supplier. Moreover the same feed compositions have been used both in cycle 6 and 7, in order to verify reproducibility of results.

Results of the tests with the membrane reactor (MR) have been evaluated in term of CO conversion, Hydrogen Recovery Factor (HRF) and hydrogen purity in the permeate, defined, respectively, as follows:

$$\text{CO conversion}\,(\%) = \frac{CO_f - CO_{out} - CO_p}{CO_f} 100$$

where C_f, C_{out} and C_p represent, respectively, CO flux measured in the feed in the retentate and in the permeate.

$$\text{HRF}\,(\%) = \frac{H_{2p}}{H_{2p} + H_{2out}} 100$$

where H_{2p} and H_{2out} represent, respectively, H_2 flux measured in the permeate and the retentate.

$$H_2\ \text{purity}\,(\%) = \frac{H_{2p}}{H_{2p} + CO_{2p} + CO_p} 100$$

where H_{2p}, CO_{2p} and CO_p represent, respectively, H_2, CO_2 and CO dry flux measured in the permeate by GC analysis.

The trend of CO conversion at the thermodynamic equilibrium, as a function of the temperature, is shown in Fig. 7, for both the syngas inlet compositions indicated in Table 3. These values represent the maximum conversions achievable with a traditional reactor (TR). Before tests with the membrane reactor, tests with the traditional reactor have been performed with both the syngas compositions. Tests have been performed at 410 °C at a pressure ranging from 250 to 300 kPa. Results are also shown in Fig. 7. A CO conversion of the 36.6% and 15.8%, for feed 1 and feed 2, respectively, has been obtained. These values are very close to the maximum achievable conversions at the thermodynamic equilibrium, thus indicating good performances of the catalyst in the specific experimental conditions.

Typical results of the syngas tests in the palladium membrane reactor, obtained during cycle 6, are shown in Figs. 8–10.

As shown in Fig. 8, while increasing the feed pressure, CO conversion increases up to 85% and 78% for feed 1 and 2, respectively, due to the hydrogen permeation through the membrane. These values can be compared with the corresponding conversions obtained with the TR, 36.6% and 15.8%, respectively, and are well above maximum conversion achievable with a TR (dotted line in the figure). Furthermore it can be noted that no methane formation has been detected by the GC analysis.

The Hydrogen Recovery Factor (HRF) and H_2 purity in the permeate, as a function of the feed pressure, are shown in Fig. 9. While increasing the feed pressure, up to the 83% of the total H_2 can be

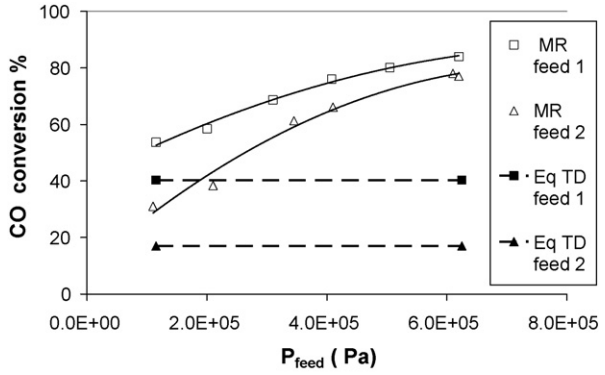

Fig. 8. CO conversion as a function of feed pressure: results of cycle 6.

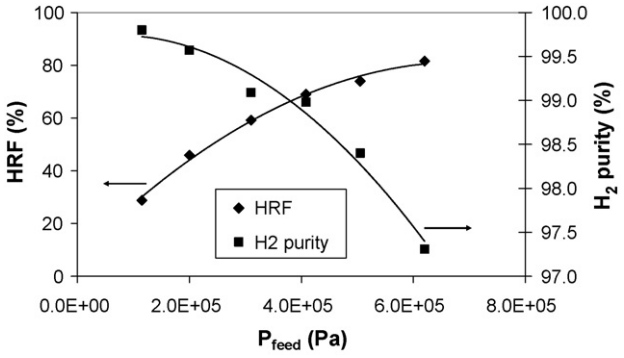

Fig. 9. Hydrogen Recovery Factor (HRF) and H_2 purity as a function of feed pressure (feed 1, cycle 6).

recovered in the permeate; purity of the recovered H_2, however, exhibits an opposite trend and decreases down to the 97.3%, due to the permeation of CO_2 through the defects in the Pd layer. Moreover HRF tends to an asymptotic value, probably due to a concentration polarization phenomena at the membrane surface, thus suggesting that reactor fluidodynamic can play an important role in determining optimum process performances. Polarization phenomena have also been evidenced by Peters and others in a recent paper [19] while testing a thin Pd–23%Ag/stainless steel composite membrane in WGS mixtures.

CO conversion as function of HRF is shown in Fig. 10. CO conversion increases linearly with HRF and presents a higher slope for the feed with a lower H_2O/CO ratio. This behaviour confirms that a membrane reactor, if properly designed, can produce high

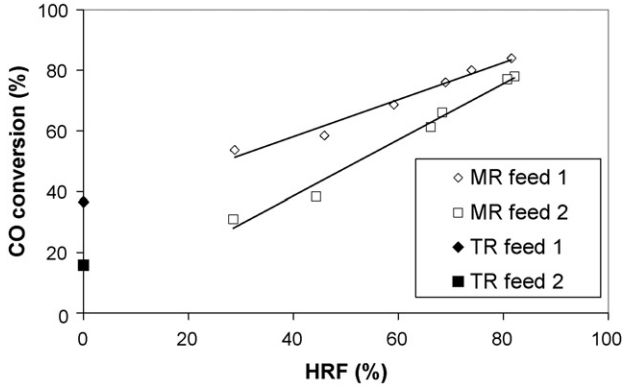

Fig. 10. CO conversion as a function of HRF: comparison of membrane reactor (MR) with traditional reactor (TR) data.

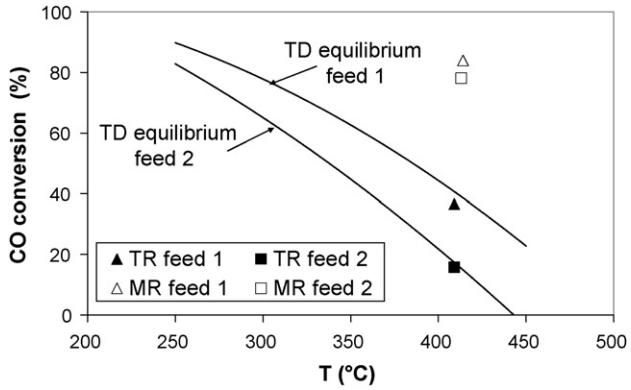

Fig. 11. CO conversion as a function of temperature: comparison of thermodynamic equilibrium values with experimental data.

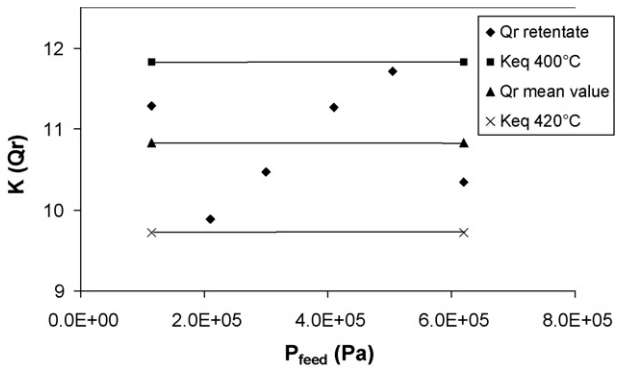

Fig. 12. Reaction quotient values (Q_r) values of the syngas at the exit of the membrane reactor: comparison with the K_{eq} value at 400 and 420 °C.

performances even at low H_2O/CO ratio, thus minimizing energy penalties connected to the WGS process in power plants.

Experimental data has been further elaborated, as shown in Fig. 11, where maximum CO conversions obtained with the membrane reactor are compared to the conversions achievable at the thermodynamic equilibrium (e.g. with a traditional reactor) in the 250–450 °C temperature range. It can be noted that the membrane reactor can achieve at 414 °C the same conversion that could be obtained, at the equilibrium, at about 260 °C. Stated that for a defined temperature there is a unique value of the equilibrium constant K_{eq}, the equilibrium shift or dynamic equilibrium reached by a membrane reactor can be quantitatively defined using the well-known concept of reaction quotient, Q_r. The reaction quotient for a membrane reactor can be calculated on the basis of the outlet composition. For a traditional fixed bed reactor Q_r should be lower or equal to K_{eq} for a defined temperature. The compositions of the syngas at the exit of the membrane reactor lead to Q_r values which lay in between the K_{eq} values at 400 and 420 °C (Fig. 12).

At the end of cycle 6 membrane performances have been checked in single gas permeation tests (H_2 and He, respectively). Hydrogen permeance has been reduced of about the 28%, while He permeance remained unchanged. Both the catalyst and the membrane have been removed from the reactor; at a visual examination the membrane surface appeared as fouled by some deposits. The membrane has been then cleaned in demineralised water in an ultrasound bath at 40 °C, for several times until the water appeared as clean; the removed particulate has been filtered and analyzed. SEM/EDS analysis (Figs. 13 and 14) indicate that the particulate is a mixture of chromium and iron oxides, e.g. the catalyst powder, and of alumina, 200–300 μm in size. Since the original size of the particles was in the 425–710 μm range, results suggest that both catalyst and inert have undergo a further fragmentation during WGS tests. Moreover no carbon has been detected on the membrane surface

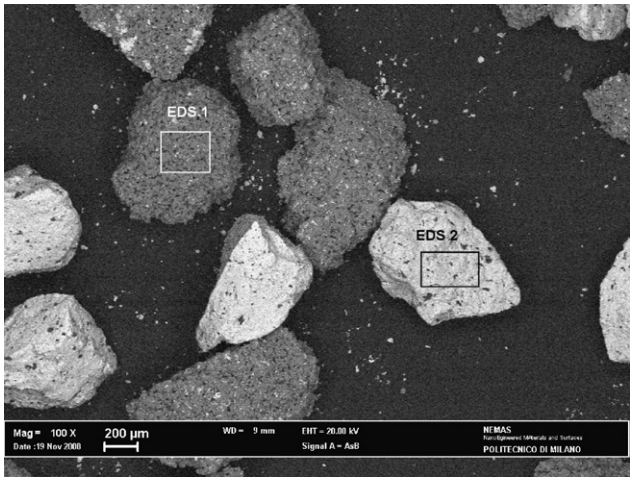

Fig. 13. SEM image in back-scattering of the deposits on the membrane surface.

by the SEM/EDS analysis: this behaviour is in good agreement with the rather high H_2O/CO ratio (3.58 and 2.66, respectively) used in the tests.

The cleaned membrane and a new catalyst have been placed in the reactor and heated up to 400 °C (cycle 7). Before WGS tests, permeation tests in pure H_2 have been performed; results indicate that the original permeance values have been restored. Concerning WGS tests, the same results as in cycle 6 have been obtained, as shown in Figs. 15 and 16, respectively, thus indicating a good reproducibility of the experimental data.

At the end of cycle 7, however, a reduction of H_2 permeance of about the 30% has been again measured (Fig. 17). The membrane has been removed from the reactor, cut in pieces and analyzed by Scanning Electron Microscope (SEM). A SEM images of the mem-

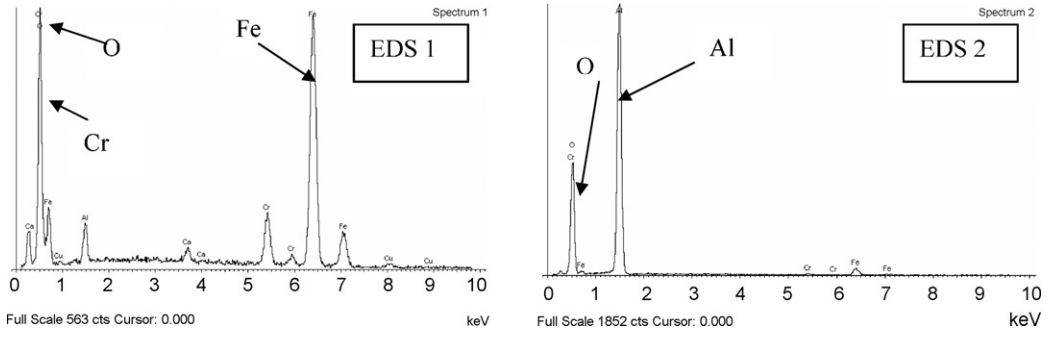

Fig. 14. EDS spectra of the deposits on the membrane surface.

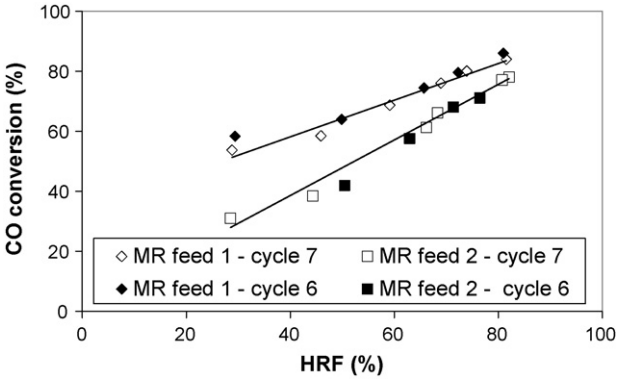

Fig. 15. CO conversion as a function of HRF: comparison of cycle 6 and cycle 7 experimental data.

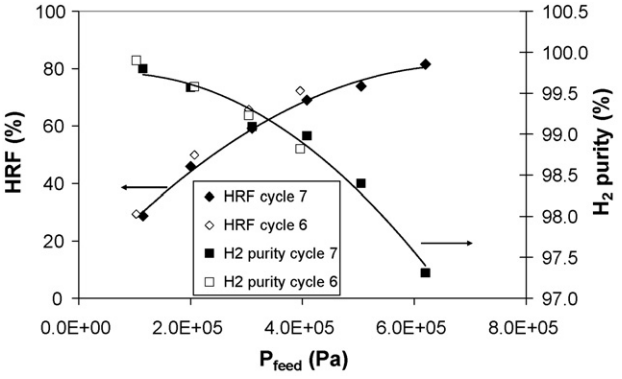

Fig. 16. Hydrogen Recovery Factor (HRF) and H_2 purity as a function of feed pressure: comparison of cycle 6 and cycle 7 experimental data obtained with feed 1.

brane surface, is shown in Fig. 18. It can be noted the characteristic cauliflower morphology of palladium clusters and the presence of other deposits on the palladium layer. Membrane samples, in correspondence of the areas where the deposits have accumulated, have been further analyzed by Auger spectroscopy coupled with sputtering by using a beam of argon ions with a kinetic energy of 4 keV and a current of 1 μA. The sample surface has been eroded for a total of 300 s, corresponding to an equivalent thickness of SiO_2 of about 5 nm; after each sputtering cycle Auger spectra have been determined. Typical results are shown in Fig. 19: the concentration of Pd rapidly grows from the 20 to the 90%, while the corresponding concentrations of chromium and oxygen follow an opposite trend and are reduced tot a few percent.

It can be concluded, therefore, that membrane fouling is determined by physical deposition of the catalyst which can be easily

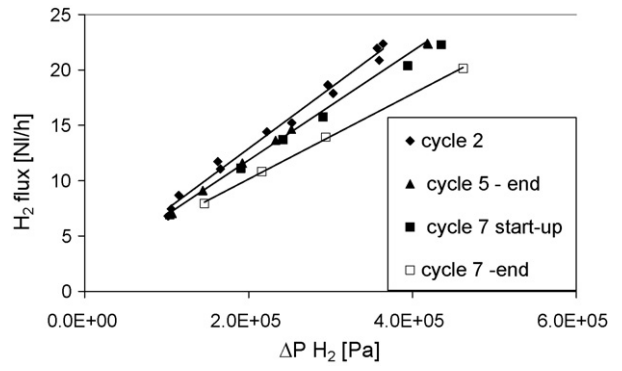

Fig. 17. Hydrogen flux measurements during the membrane life.

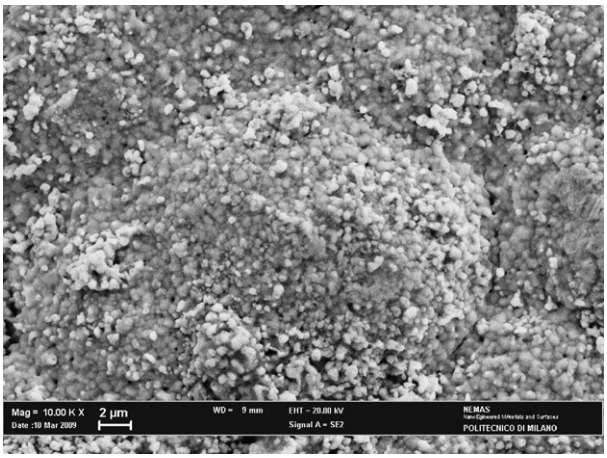

Fig. 18. SEM image of the surface of the membrane at the end of the WGS tests.

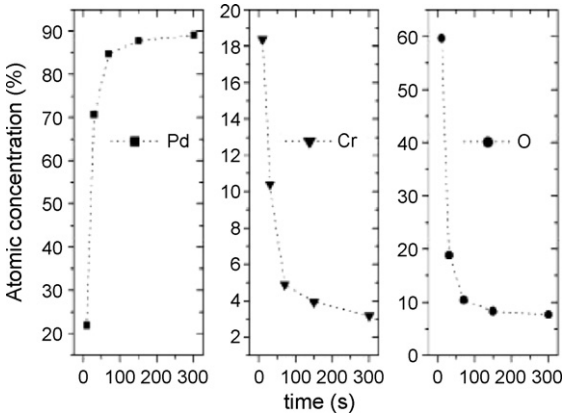

Fig. 19. Atomic concentration of Pd Cr, and O measured at different sputtering times by Auger spectroscopy on the surface of the membrane in correspondence of deposit accumulation.

removed by a cleaning in a ultrasound bath. The observed phenomena appears related to the experimental asset, e.g. to the fact that catalyst powders have undergo a further fragmentation during WGS tests: this phenomena could not be observed in a reactor of bigger size where dimensional stable catalysts pellets could be used.

4. Conclusions

The water gas shift (WGS) reaction of a syngas mixture has been carried out in a tubular palladium membrane reactor at a temperature of 410–414 °C. A composite palladium-porous stainless steel membrane, 29 μm thick, obtained by electroless plating, has been first extensively tested with pure gases (H_2, He, CO_2) and syngas mixtures in the 310–455 °C temperature range and in the 100–800 kPa feed pressure range. Long-term stability of the membrane in H_2 at 400 °C has also been checked over a period of 1200 h. The membrane has been then used for WGS tests in a membrane reactor. The membrane reactor, packed with a Fe/Cr commercial catalyst has been operated at a reaction pressure of 100–600 kPa in the counter-current mode, with a nitrogen sweep-gas. The reactor has been fed with a shift gas mixture with a 7.6% CO concentration and H_2O/CO ratio in the 2.7–3.6 range. The membrane reactor was able to achieve up to the 85.0% of CO conversion, while only 35%, as a maximum, was reached with the traditional reactor in the same operating conditions. Up to the 82% of hydrogen has been recovered with a purity exceeding the 97%.

Acknowledgements

This work has been financed by the Research Fund for the Italian Electrical System under the Contract Agreement between the Ministry of Economic Development – General Directorate for Energy and Mining Resources and ERSE S.p.A. (formerly CESI RICERCA). We also thank G. Vanacore and M. Zani, Dipartimento di Fisica of Politecnico di Milano, who performed Auger spectroscopy analysis.

References

[1] P. Middleton, P. Hurst, G. Walker, Grace: Pre-Combustion De-Carbonization Hydrogen Membrane Study, in: D.C. Thomas, S.M. Benson (Eds.), vol. 1, Elsevier, 2005 (Chapter 27).
[2] P. Chiesa, G. Manzolini, F. Vigano, P. Savoldelli, P. Pinacci, L. Mazzocchi, Proc. of GHGT8, Trondheim (NO), June 18–23, 2006.
[3] J.V. Dijkstra, Y.C. van Delft, D. Jansen, P. Pex, Proc. of GHGT 8, Trondheim (NO), June 18–23, 2006.
[4] R. Bredesen, K. Jordal, O. Bolland, Chem. Eng. Process. 43 (2004) 1129–1158.
[5] Y.H. Ma, Proc. of ICIM 9, Lillehammer (NO), June 25–29, 2006.
[6] S.E. Nam, K.H. Lee, J. Membr. Sci. 192 (2001) 1977.
[7] B. McCool, G. Xomeritakis, Y.S. Lin, J. Membr. Sci. 161 (1999) 67–76.
[8] N. Itoh, T. Akiha, T. Sato, Catal. Today 104 (2005) 231.
[9] J.P. Collins, J.D. Way, Ind. Eng. Chem. Res. 32 (1993) 3006–3013.
[10] Y.S. Cheng, K.L. Yeung, J. Membr. Sci. 182 (2001) 195–203.
[11] I.P. Mardilovich, Y. She, Y.H. Ma, M.H. Rei, AIChE J. 44 (1998) 310–322.
[12] S.K. Gade, M.K. Keeling, D.K. Steele, J.D. Way, P.M. Thoen, Proc. of ICIM 9, Lillehammer (NO), June 25–29, 2006.
[13] A. Basile, G. Chiappetta, S. Tosti, V. Violante, Sep. Purif. Technol. 25 (2001) 549–571.
[14] S. Tosti, A. Basile, G. Chiappetta, C. Rizzello, V. Violante, Chem. Eng. J. 93 (1) (2003) 23–30.
[15] B. Arstad, H. Venvik, H. Klette, J.C. Walmsley, W.M. Tucho, R. Holmestad, H. Holmen, R. Bredesen, Catal. Today 118 (2006) 63–72.
[16] P. Pinacci, M. Broglia, M. Radaelli, A. Bottino, G. Capannelli, A. Comite, Proc. of 3rd Int. Conf. on Clean Coal Technologies for our Future, Cagliari (I), May 15–17, 2007.
[17] A. Li, W. Liang, R. Hughes, J. Membr. Sci. 165 (2000) 135–141.
[18] A. Unemoto, A. Kaimai, K. Sato, T. Otake, K. Yashiro, J. Mizusaki, T. Kawada, T. Tsuneki, Y. Shirasaki, I. Yasuda, Int. J. Hydrogen Energy 32 (2007) 2881–2887.
[19] T.A. Peters, M. Stange, H. Klette, R. Bredesen, J. Membr. Sci. 316 (2008) 119–127.
[20] S. Uemiya, N. Sato, H. Ando, E. Kikuchi, Ind. Eng. Chem. Res. 30 (1991) 589–591.
[21] Y. Bi, H. Xu, W. Li, A. Goldbach, Int. J. Hydrogen Energy 34 (2009) 2965–2971.
[22] S. Tosti, A. Basile, L. Bettinali, F. Borgognoni, F. Chiaravalloti, F. Gallucci, J. Membr. Sci. 284 (2006) 393–397.
[23] A. Matzakos, Presentation at the 2006 NHA Annual Meeting – Fuel Cells Topical – Innovations in Fuel Processing Session, 2006.
[24] M.V. Mundschau, X. Xie, C.R. Evenson, A.F. Sammels, Catal. Today 118 (2006) 12–23.
[25] T.A. Peters, W.M. Tucho, A. Ramachandran, M. Stange, J.C. Walmsley, R. Holmestad, A. Borg, R. Bredesen, J. Membr. Sci. 326 (2009) 572–581.
[26] Y.H. Ma, M.E. Ayturk, A.S. Augustine, N.K. Kazantzis, Proc. of ICCMR 9, Lyon (Fr), 28 Giu–2 July, 2009.
[27] I.P. Mardilovich, E. Engwall, Y.H. Ma, Desalination 144 (2002) 85–89.
[28] M. Broglia, P. Pinacci, M. Radaelli, A. Bottino, G. Capannelli, A. Comite, G. Vanacore, M. Zani, Desalination 245 (2009) 508–515.
[29] Y.H. Ma, J.P. Mardilovich, Y. She, US Patent 6,152,987, November 28, 2000.
[30] K.S. Rothenberger, A.V. Cugini, B.H. Howard, R.P. Killemeyer, M.V. Ciocco, B.D. Morreale, R.M. Enick, F. Bustamante, I.P. Mardilovich, J. Membr. Sci. 244 (2004) 55–68.
[31] F. Guazzone, E.E. Engwall, Y.H. Ma, Catal. Today 118 (2006) 24–31.
[32] B.D. Morreale, M.V. Ciocco, R.M. Enick, B.I. Morsi, B.H. Howard, A.V. Cugini, K.S. Rothenberger, J. Membr. Sci. 212 (2003) 87–97.
[33] F. Guazzone, Engineering of substrate surface for the synthesis of ultra-thin composite Pd and Pd–Cu membranes for hydrogen separation, PhD Thesis, WPI (USA), December 2005.
[34] A. Bottino, G. Capannelli, A. Comite, R. Di Felice, M. Broglia, P. Pinacci, Proc. of ICIM 9, Lillehammer (NO), June 25–29, 2006.